Journal of Molecular Structure 1101 (2015) 139–146

Contents lists available at ScienceDirect

Journal of Molecular Structure

journal homepage: http://www.elsevier.com/locate/molstruc

Synthesis, characterization and biological activities of metal(II) dipicolinate complexes derived from pyridine-2,6-dicarboxylic acid and 2-(piperazin-1-yl)ethanol

Nurgün Büyükkıdan [a, *], Cengiz Yenikaya [a], Halil İlkimen [a], Ceyda Karahan [a], Cihan Darcan [b], Tülin Korkmaz [c], Yasemin Süzen [d]

[a] Department of Chemistry, Faculty of Arts and Science, Dumlupınar University, 43100 Kütahya, Turkey
[b] Department of Molecular Biology and Genetic, Faculty of Arts and Science, Bilecik Şeyh Edebali University, Bilecik, Turkey
[c] Department of Molecular Biology and Genetic, Institue of Science, Bilecik Şeyh Edebali University, Bilecik, Turkey
[d] Department of Chemistry, Faculty of Arts and Science, Anadolu University, 26470, Eskişehir, Turkey

ARTICLE INFO

Article history:
Received 13 March 2015
Received in revised form
5 August 2015
Accepted 5 August 2015
Available online 8 August 2015

Keywords:
Pyridine-2,6-dicarboxylic acid
2-(piperazin-1-yl)ethanol
Metal(II) complex
Water cluster
Antimicrobial activity

ABSTRACT

The new water-soluble and air stable compounds $(H_2ppz)[Co(dipic)_2]\cdot 6H_2O$ (**1**), $(H_2ppz)[Ni(dipic)_2]\cdot 6H_2O$ (**2**) and $(H_2ppz)[Zn(dipic)_2]\cdot 6H_2O$ (**3**) were prepared by the reaction of corresponding metal(II) acetates and a proton transfer salt, $(H_2ppz)(Hdipic)_2$, (**4**) of pyridine-2,6-dicarboxylic acid (H_2dipic) and 2-(piperazin-1-yl)ethanol (ppz). The compounds **1**–**3** were characterized by elemental, IR, UV–vis. thermal analyses, magnetic measurement and single crystal X-ray diffraction studies. The molecular structures of the title compounds consist of one 1-(2-hydroxyethyl)piperazine-1,4-diium (H_2ppz^{+2}) cation, one bis(pyridine-2,6-dicarboxylate)metal(II) $[M(dipic)_2]^{2-}$ anion, and six uncoordinated water molecules. In compounds **1**–**3** the metal ions coordinate to two oxygen and one nitrogen atoms of two pyridine-2,6-dicarboxylate molecules forming an octahedral environment. Antimicrobial activities against Gram (−) wild type (*Escherichia coli* and *Pseudomonas aeruginosa*), Gram (+) wild type (*Staphylococcus aureus, Staphylococcus epidermidis, Bacillus cereus* and *Bacillus subtilis*) and clinical isolate (*Morganella morganii*, *Proteus vulgaris and Enterobacter aeruginosa*) were also studied. The results were reported, discussed and compared with the corresponding starting materials ($(H_2ppz)(Hdipic)_2$ (**4**), H_2dipic and ppz). MIC (Minimal Inhibition Concentration) values of the newly synthesized compounds were determined as 4000 μg/ml (except *B. subtilis* and clinical isolate *E. aeruginosa*, >4000 μg/ml).

1. Introduction

Pyridine-2,6-dicarboxylic acid (H_2dipic) is a fully acknowledged structural component in many metal-organic frameworks [1–8] in biochemistry and in the formation of water clusters [9–15]. For chemical systems, the degree of structuring of water cluster can be of importance for the design as well as the stabilization of new structures [16]. H_2dipic has a rigid 120° angle between the central pyridine ring and two carboxylate groups. Proton donating and accepting capabilities for hydrogen bonding via the oxygen atoms of its carboxylate groups [17] provide various coordination modes to form both discrete and polymeric metal complexes under an appropriate synthesis condition [2].

Metal complexes of H_2dipic and some of their derivatives have shown antimicrobial activities in recent years [18,19]. The enhancement of the antimicrobial activity of certain chemicals can be achieved by the addition of metals. The role of metals in antimicrobial activity is shown in many studies [20–24].

The metal complexes with mixed ligands of these compounds have shown better biological activities than the simple ones [25–29]. Continuing the path to synthesize proton transfer compounds, our group has focused on forming ion pairs between H_2dipic and various organic bases, such as 2-aminobenzothiazole [30], 2-amino-6-chlorobenzothiazole [29], 2-amino-6-methylbenzothiazole [31], 2-amino-6-methoxybenzothiazole [32], 2-amino-4-methylpyridine [26], 2-(piperazin-1-yl)ethanol (ppz) [18].

In this study, we report three new compounds (H_2ppz)

* Corresponding author.
E-mail address: nurgun.buyukkidan@dpu.edu.tr (N. Büyükkıdan).

http://dx.doi.org/10.1016/j.molstruc.2015.08.015
0022-2860/

$[Co(dipic)_2].6H_2O$ (**1**), $(H_2ppz)[Ni(dipic)_2].6H_2O$ (**2**) and $(H_2ppz)[Zn(dipic)_2].6H_2O$ (**3**) of a proton transfer salt $(H_2ppz)(Hdipic)_2$ (**4**) (H_2ppz = 1-(2-hydroxyethyl)piperazine-1,4-diium). The characterization has been made by using elemental and thermal analysis, magnetic measurement, IR and UV–vis electronic spectra of the compounds (**1**–**3**). The molecular structures of **1**–**3** were elucidated by a single crystal X-ray diffraction studies.

2. Experimental

2.1. Materials

All chemicals used were of analytical grade purchased from Aldrich. ^{1}H NMR spectra were recorded by 500 MHz UltraShield NMR spectrometer ($SiMe_4$ as internal standard and 85% H_3PO_4 as an external standard). Elemental analyses for C, H and N were performed on a Leco CHNS-932 instrument. IR spectra were recorded on a Bruker Optics, vertex 70 FT-IR spectrometer using ATR techniques. Thermal analyses were performed on SII Exstar 6000 TG/DTA 6300 model using platinum crucible with 10 mg sample. TG/DTA measurements were taken in static air within a 30–700 °C temperature range. The UV–vis spectra were carried out with a SHIMADZU UV-2550 spectrometer in the range 900–200 nm. Magnetic susceptibility measurements at room temperature were taken using a Sherwood Scientific Magway MSB MK1 model magnetic balance by the Gouy method using Hg $[Co(SCN)_4]$ as calibrant. Molar conductance of the compounds was determined in DMSO (10^{3-} M) at room temperature using a WTW Cond 315i/SET Model conductivity meter.

2.2. Synthesis of compounds (*1*–*3*)

The proton transfer salt $(H_2ppz)(Hdipic)_2$ (**4**) was prepared according to the method reported previously [18].

A solution of 1 mmol of a metal(II) salt [0.249 g $Co(CH_3COO)_2.4H_2O$ or 0.248 g $Ni(CH_3COO)_2.4H_2O$ or 0.220 g $Zn(CH_3COO)_2.2H_2O$] in water (10 mL) was added dropwise to the solution of **4** (0.462 g, 1 mmol) in water (10 mL) with stirring at room temperature for 2 h. The reaction mixture was kept at room temperature for two weeks to give purple crystalline solid for **1** (0.378 g, 60% yield), green crystalline solid for **2** (0.409 g, 65% yield), and colourless crystalline solid for **3** (0.445 g, 70% yield) (Scheme 1). The single crystals of all compounds suitable for X-ray diffraction were separated and washed with water.

Elemental analysis for the compounds **1**–**3** are as follows:

Anal. Calcd. for **1** ($C_{20}H_{34}N_4O_{15}Co$): C, 38.16%; H, 5.44%; N, 8.90%; Co, 9.36%, Found: (%): C, 37.97%; H, 5.28%; N, 8.80%; Co, 9.30%. Anal. Calcd. for **2** ($C_{20}H_{34}N_4O_{15}Ni$): C, 38.18%; H, 5.45%; N, 8.90%; Ni, 9.33% Found: C, 37.78%; H, 5.28%; N, 8.77%; Ni, 9.30%. Anal. Calcd. for **3** ($C_{20}H_{34}N_4O_{15}Zn$): C, 37.78%; H, 5.39%; N, 8.81%; Zn, 10.28%, Found: C, 37.31%; H, 5.22%; N, 8.63%; Zn, 10.30%.

2.3. X-ray crystal structure determination

The crystallographic data are given in Table 1; the selected bond lengths and angles are listed in Table 2; and the hydrogen-bond geometries are given in Tables S1–S4 for the compounds **1**–**3**. Intensity data were recorded on a Bruker Kappa APEXII CCD area-detector diffractometer using Mo K_α radiation (λ = 0.71073 Å) at T = 100(2) K. Absorption corrections by multi-scan [33] were applied. Structures were solved by direct methods and refined by full-matrix least squares against F^2 using all data [34]. All non-H atoms were refined anisotropically. In compounds **1**, **2** and **3**, atoms H10A, H10B, H11A, H11B, H12A, H12B, H13A, H13B, H14A, H14B, H15C, H15D (H_2O), H33A, H33B (NH_2) and H44 (NH) were located in difference Fourier maps and were freely refined. The

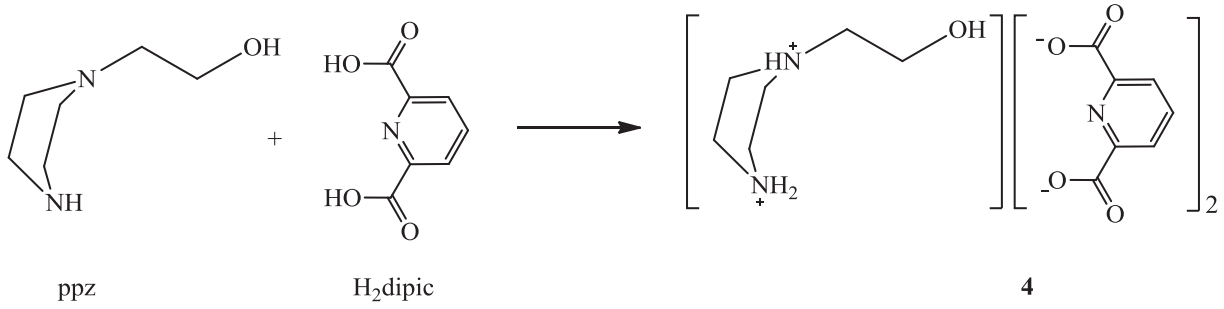

(a)

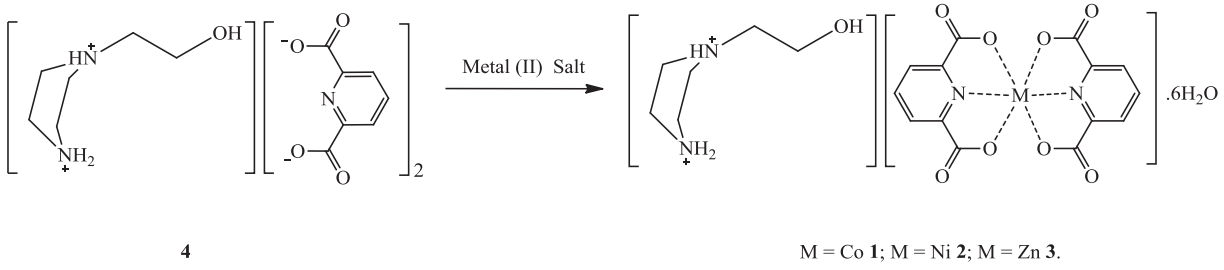

(b)

Scheme 1. Syntheses of compounds **1**–**4** (**a** for **4** and **b** for **1**–**3**).

Table 1
Crystallographic details for compounds **1**, **2** and **3**.

Compound	**1**	**2**	**3**
Chemical formula	$C_{20}H_{34}N_4O_{15}Co$	$C_{20}H_{34}N_4O_{15}Ni$	$C_{20}H_{34}N_4O_{15}Zn$
FW/g mol^{-1}	629.44	629.20	635.90
Crystal System	monoclinic	monoclinic	monoclinic
Space group	$P2_1/c$	$P2_1/c$	$P2_1/c$
a/Å	12.0728(2)	11.8475(3)	12.1156(4)
b/Å	17.7903(3)	17.9158(4)	17.7872(6)
c/Å	13.2960(2)	13.2610(3)	13.3058(4)
β/°	114.402(1)	112.813(3)	114.726(1)
V/Å^3	2600.60(8)	2594.56(12)	2604.54(15)
Z	4	4	4
ρ_{calc}mg/mm^3	1.608	1.611	1.622
μ(Mo-Kα)/mm^{-1}	0.742	0.831	1.025
F(000)	1316.0	1320.0	1328.0
Crystal size/mm^3	0.35 × 0.25 × 0.15	0.29 × 0.26 × 0.21	0.28 × 0.24 × 0.10
2Θ range for data collection	4.06–56.88°	4.36–56.84°	4.08–56.76°
Reflections collected	23962	24562	44156
Independent reflections	6498[R(int) = 0.0240]	6486[R(int) = 0.0337]	6475[R(int) = 0.0353]
Data/restraints/parameters	6498/10/416	6486/8/419	6475/15/421
Goodness-of-fit on F^2	1.109	1.049	1.031
Final R indexes [$I \geq 2\sigma$ (I)]	$R_1 = 0.0330$, $wR_2 = 0.0930$	$R_1 = 0.0321$, $wR_2 = 0.0797$	$R_1 = 0.0285$, $wR_2 = 0.0693$
Final R indexes [all data]	$R_1 = 0.0388$, $wR_2 = 0.0976$	$R_1 = 0.0416$, $wR_2 = 0.0850$	$R_1 = 0.0382$, $wR_2 = 0.0737$
Largest diff. peak/hole/e Å^{-3}	0.662/−0.708	0.666/−0.436	0.699/−0.587

atoms H9 (OH) and the C-bound H-atoms were positioned geometrically at the distances of 0.82 Å (OH), 0.93 Å (CH) and 0.97 Å (CH_2) from the parent atoms; a riding model was used during the refinement process and the U_{iso}(H) values were constrained to be nU_{eq}(carrier atom), where n = 1.5 for OH H-atoms and n = 1.2 for all other H-atoms.

2.4. Antimicrobial assay

Gram-negative bacteria *Escherichia coli* W3110, *Pseudomonas aeruginosa* ATCC 27853, gram-positive bacteria *Staphylococcus aureus* ATCC6535, *Bacillus cereus* ATCC7064, *Staphylococcus epidermidis* ATCC 12228, *Bacillus subtilis*, and clinical isolate of *Morganella morganii, Proteus vulgaris, Enterobacter aeruginosa* were used in this study to test the antimicrobial activity of new metal compounds. Antimicrobial activity tests were carried out using the

Table 2
Selected bond lengths (Å) and angles (°) for compounds **1**, **2** and **3**.

Complex 1		Complex 2		Complex 3	
Co1–O2	2.1517(13)	Ni1–O2	2.1108(12)	Zn1–O2	2.1279(11)
Co1–O3	2.1489(14)	Ni1–O3	2.1402(12)	Zn1–O3	2.2413(11)
Co1–O6	2.1404(13)	Ni1–O6	2.1312(12)	Zn1–O6	2.1427(11)
Co1–O7	2.1724(13)	Ni1–O7	2.1172(12)	Zn1–O7	2.2074(11)
Co1–N1	2.0211(15)	Ni1–N1	1.9642(15)	Zn1–N1	2.0229(13)
Co1–N2	2.0243(15)	Ni1–N2	1.9601(14)	Zn1–N2	2.0205(13)
O1–C1	1.247(2)	O1–C1	1.240(2)	O1–C1	1.247(2)
O2–C1	1.265(2)	O2–C1	1.271(2)	O2–C1	1.266(2)
O4–C7	1.239(2)	O4–C7	1.248(2)	O4–C7	1.244(2)
O5–C8	1.247(2)	O5–C8	1.250(2)	O5–C8	1.246(2)
O6–C8	1.267(2)	O6–C8	1.263(2)	O6–C8	1.267(2)
O8–C14	1.239(2)	O8–C14	1.238(2)	O8–C14	1.240(2)
O9–C20	1.413(2)	O9–C20	1.416(2)	O9–C20	1.414(2)
C1–C2	1.520(2)	C1–C2	1.514(2)	C1–C2	1.518(2)
C6–C7	1.513(3)	C6–C7	1.520(2)	C6–C7	1.522(2)
C9–C8	1.517(3)	C9–C8	1.519(2)	C9–C8	1.516(2)
C14–C13	1.517(2)	C14–C13	1.517(2)	C14–C13	1.517(2)
O2–Co1–O3	152.40(5)	O2–Ni1–O3	155.86(5)	O2–Zn1–O3	152.63(4)
O2–Co1–O6	96.56(5)	O2–Ni1–O6	90.47(5)	O2–Zn1–O6	99.24(4)
O2–Co1–O7	90.83(5)	O2–Ni1–O7	93.03(5)	O2–Zn1–O7	90.09(4)
O6–Co1–O3	90.01(5)	O6–Ni1–O3	95.59(5)	O6–Zn1–O3	90.20(4)
O6–Co1–O7	152.61(5)	O6–Ni1–O7	156.39(5)	O6–Zn1–O7	152.53(4)
O7–Co1–O3	95.57(5)	O7–Ni1–O3	90.70(5)	O7–Zn1–O3	93.22(4)
N1–Co1–O2	76.77(6)	N1–Ni1–O2	77.73(5)	N1–Zn1–O2	77.91(5)
N1–Co1–O3	75.78(6)	N1–Ni1–O3	78.13(5)	N1–Zn1–O3	74.75(5)
N1–Co1–O6	109.96(6)	N1–Ni1–O6	104.38(5)	N1–Zn1–O6	112.45(5)
N1–Co1–O7	97.39(5)	N1–Ni1–O7	99.18(5)	N1–Zn1–O7	94.71(5)
N2–Co1–O2	111.63(6)	N2–Ni1–O2	97.60(5)	N2–Zn1–O2	111.60(5)
N2–Co1–O3	95.97(6)	N2–Ni1–O3	106.50(5)	N2–Zn1–O3	95.47(5)
N2–Co1–O6	77.00(6)	N2–Ni1–O6	78.40(5)	N2–Zn1–O6	77.58(5)
N2–Co1–O7	75.75(6)	N2–Ni1–O7	77.99(5)	N2–Zn1–O7	74.96(5)
N2–Co1–N1	168.90(6)	N2–Ni1–N1	174.49(6)	N2–Zn1–N1	165.57(5)

broth dilution method as described by the NCCSL standards [35] (NCCLS 2006) and disc diffusion test. All stock solutions of the compounds were prepared in pure water according to the required concentrations for experiments. The solubility of compounds is improved by heating the water bath.

3. Results and discussion

3.1. Crystal structures

The X-ray crystal structures reveal that **1**, **2** and **3** crystallize in the same space group and have closely related structures. Their asymmetric units contain one 1-(2-hydroxyethyl)- piperazine-1,4-diium cation (H_2ppz^{+2}), one bis(pyridine-2,6-dicarboxylate)metal(II) ($dipic^{2-}$) anion, and six uncoordinated water molecules. The molecular structures of compounds **1-3** are given in Figs. 1–3, respectively. The M(II) ions are six-coordinated by two tridentate $dipic^{2-}$ anions in the anionic parts of the compounds. In compounds **1**–**3**, the M(II) ions have MN_2O_4 coordinations with distorted octahedral geometries. The bond angles around the M(II) ions involving *trans* pairs of donor atoms are in the ranges of 90.01(5)°–168.90(6)° for **1**, 90.47(5)°–174.49(6)° for **2**, and 90.09(4)°–165.57(5)° for **3** deviating from linearity. The bond angles for the *cis*-pairs of donor atoms the ranges are 75.75(6)°–152.61(5)° for **1**, 77.73(5)°–156.39(5)° for **2**, and 74.75(5)°–152.63(4)° for **3** (Table 2). These angular values indicate a large distortion from the ideal octahedral geometry due to the binding of the $dipic^{2-}$ ligands to the M(II) ions in tridentate manner. The M–O and M–N bonds (Table 2) are in the normal ranges. In **1**, two of the crystal water molecules (O12 and O15) are involved in intermolecular hydrogen-bondings with the carboxyl oxygen atoms (O1 and O5) of the $dipic^{2-}$ ligand. There are also intermolecular hydrogen-bondings between the two crystal water molecules (O12 and O13) and between one of the crystal water molecules (O14) and one of the nitrogen atoms (N3) of the H_2ppz^{+2} cation (Table S1). In **2**, one of the crystal water molecules (O12) is involved in intermolecular hydrogen-bonding with the carboxylate oxygen atom (O2) of the $dipic^{2-}$ ligand. There are also intermolecular hydrogen-bondings between the crystal water molecules (O10, O12 and O13) and between (O14 and O15) (Table S2). In **3**, one of the crystal water molecules (O12) is involved in intermolecular hydrogen-bonding with the carboxylate oxygen atom (O5) of the dipic ligand. There are also intermolecular hydrogen-bonding between the crystal water molecules (O11 and O12) (Table S3). In **1**–**3**, all the $dipic^{2-}$ ligands are planar and they are oriented one towards another at the dihedral angles of 87.10(2)° (for **1**), 87.57(2)° (for **2**), and 87.39(2)° (for **3**). In the crystal structure, intermolecular N–H···O, O–H···O hydrogen bonds (Tables S1–S3) link the molecules into supramolecular networks as well as the van der Waals interactions between C–H O ranged 2.40–2.60 **Å** (Table S4).

Compound **1** has a pentamer water cluster (Fig. 1). In this cluster, O15 interacts with H_2ppz^{2+} ligand as hydrogen-bonding acceptor and O10 interacts as hydrogen-bonding donor to $dipic^{2-}$ ligand. H_2ppz^{2+} and $dipic^{2-}$ ligands are linked together by O12. The water molecules are strongly hydrogen-bonded to each other as well as to the nearby O atoms (O1 and O5) of the carboxylate and H_2ppz^{2+} groups. The hydrogen bonding parameters pertaining to the water cluster are collected in Table S1.

Interestingly, the crystal structure of **2** (Fig. 2) has a cyclic water tetramer. In this structure, H_2ppz^{2+} and $dipic^{2-}$ ligands are connected together by the linkage of water molecules, O14 and $O13^a$ (members of tetramer ring), and $O12^a$. The other water molecules, ($O10^a$ and O15), are only the members of the tetramer ring which is fully coplanar. The O–H···O angles (166(4) and 168(3)^0) within the water tetramer are larger than those observed in [(Bpyph)SCN_2].$2H_2O$ (159.1(4) and 156.7(4)^0), and four hydrogen atoms are out of the plane constructed by four oxygen atoms. O13–H13A … O14 angle (130(4)) is very small because of the water–water (O13–O12) interaction, although the O … O distances ranging from 2.72(3) to 2.83(2) Å in the tetramer are comparable to the reported tetramer (2.68–2.76 Å) [36]. These arrangements give rise to four member rings which can be described as R_4^4 (4) in 1D chain, and which play an important role in the stabilization of crystal structure (Table S2).

A notable feature of hydrogen-bonding assemblies of **3** is the presence of pentameric $(H_2O)_5$ water cluster (Fig. 3). This cluster is stabilized in the crystal structure by strong hydrogen bonding interactions. This pentamer connects two H_2ppz^{2+} moieties by using $O12^d$ and $O14^e$ atoms to form hydrogen-bonding. On the other hand, one H_2ppz^{2+} ring is directly connected to carboxylate oxygen ($O4^h$) as hydrogen-bonding donor, and the other H_2ppz^{2+} ring interacts with carboxylate oxygen ($O4^h$) via water ($O13^i$) bridge by strong hydrogen bonds. The hydrogen bonding parameters pertaining to the water clusters are presented in Table S3.

3.2. FT-IR spectra

The IR spectra of compounds **1**, **2** and **3** were determined within the 4000-400 cm^{-1} frequency range, and the significant frequencies in the IR spectra of synthesized compounds **1**–**3** and proton transfer salt (**4**) are given in Table S5. The IR spectra of compounds are characterized by a broad band at 3468 cm^{-1} for **1**, 3469 cm^{-1} for **2** and 3465 cm^{-1} for **3**, which can be ascribed to the ν(O–H) stretching vibration of water molecules present in the lattice, which is consistent with the elemental and crystal structure analyses. The stretching ν(N–H) vibrations of amine groups are observed at 3219, 3210 and 3173 cm^{-1} for compounds **1**, **2**, and **3**, respectively. The relatively weak bands at 3092 and 3015 cm^{-1} for compounds **1**, 3093 and 3015 cm^{-1} for **2** and 3097 cm^{-1} for **3** are due to the aromatic ν(C–H) vibrations. Aliphatic ν(C–H) stretching vibrations are observed at 2760 and 2762 cm^{-1} for compounds **1** and **2**, respectively, but not for compound **3** due to the overlapping with broad ν(O–H) vibration band. There are very strong bands at 1609 and 1571 cm^{-1} for all compounds which are typical for asymmetric and symmetric ν(COO) vibrations of coordinated carboxylate groups [19]. The weak bands are at 591 and 423 cm^{-1} for **1**, 592 and 426 cm^{-1} for **2**, and 588 and 428 cm^{-1} for **3**, respectively, which are due to ν(M–O) and ν(M–N) vibrations.

3.3. Thermal analysis

Figs. S1–S3 show the TG-DTG and DTA curves of compounds **1**, **2** and **3**, respectively. The compounds (**1**–**3**) were thermally decomposed in three steps (Table S6). For compound **1**, the first stage (DTGmax = 103 °C) originates from an endothermic peak observed between 30 and 135 °C and corresponds to the loss of 6 mol of hydrate water molecules (found 17.10, calcd. 17.16%). The exothermic second stage (DTGmax = 306, 318 °C), between 135 and 340 °C, corresponds to the loss of the $C_{14}H_{22}N_2O$ group of the H_2ppz^{2+} ligand (found 37.20, calcd. 37.24%). The exothermic third stage, a loss of $C_6N_2O_8$ of $dipic^{2-}$ residue is observed between 304 and 650 °C with DTG_{max} at 368 °C (found 36.40, calcd. 36.24%). The final decomposition product was CoO identified by IR spectroscopy (found 9.30%, Calcd 9.36%).

For the compound **2**, the first stage (DTGmax = 78 °C) originates from an endothermic peak observed between 30 and 115 °C and corresponds to the loss of 6 mol of hydrate water molecules (found 16.90, calcd. 17.17%). The exothermic second stage (DTGmax = 278,

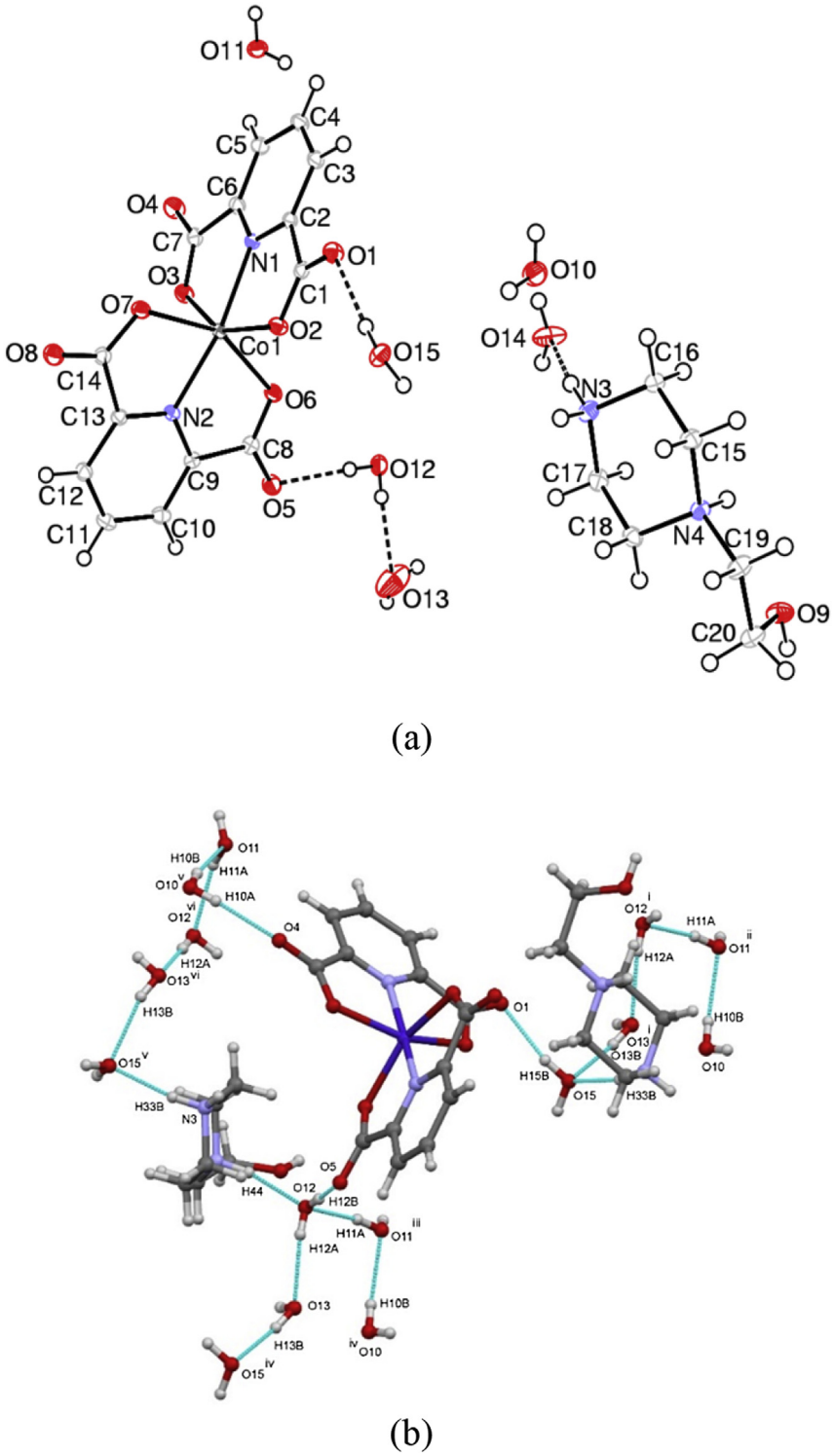

Fig. 1. (a) The molecular structure of compound **1** with the atom-numbering scheme. Displacement ellipsoids are drawn at a 50% probability level. The intermolecular O–H···O hydrogen bonds are shown as dashed lines. (b) A perspective view of the $(H_2O)_5$ cluster i; −1 + x, y, z ii; −1 + x, 3/2 − y, −1/2 + z iii; x, 3/2 − y, −1/2 + z, iv; 1 + x,y,z v; 1 + x, 3/2 − y, 1/2 + z vi; x, 3/2 − y, 1/2 + z.

298, 308 °C) between 115 and 353 °C, is consistent with the loss of the $C_{10}H_{20}N_2O$ group from the H_2ppz^{2+} ligand (found 30.50, calcd. 29.29%). The exothermic third stage, (DTG_{max} = 382, 422 °C) between 353 and 600 °C, is consistent with the loss of the $C_{10}H_2N_2O_8$ from $dipic^{2-}$ residue in compound **2** (found 43.32, calcd. 44.21%). The final decomposition product was NiO identified by IR spectroscopy (found 9.28%, Calcd 9.33%).

For the compound **3**, the first stage (DTGmax = 75 °C) originates from an endothermic peak observed between 30 and 115 °C and corresponds to the loss of 6 mol of hydrate water molecules (found 16.90, calcd. 16.98%). The exothermic second stage (DTGmax = 285 °C), between 115 and 290 °C, corresponds to the

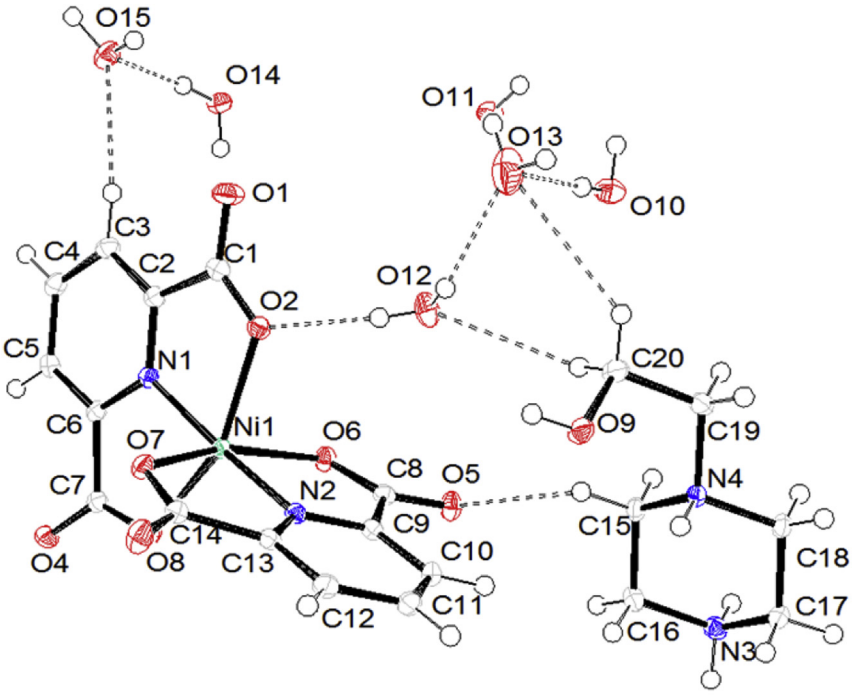

(a)

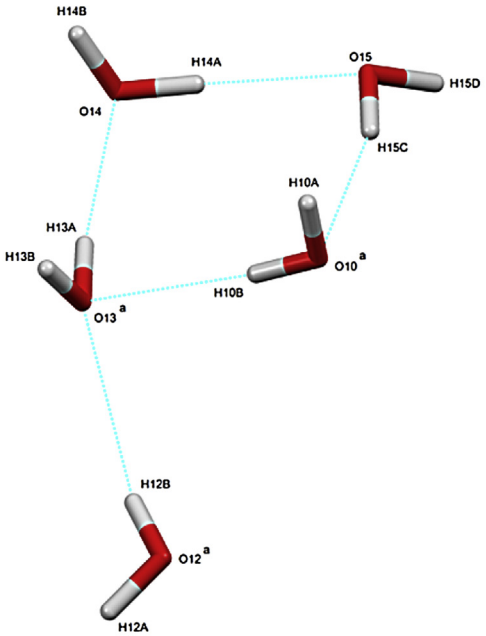

(b)

Fig. 2. (a) The molecular structure of compound **2** with the atom-numbering scheme. Displacement ellipsoids are drawn at a 50% probability level. The intermolecular O–H···O hydrogen bonds are shown as dashed lines. (b) A perspective view of the $(H_2O)_4$ cluster a; 1 − x, −y, 1 − z.

loss of the $C_{14}H_{24}N_2O$ group of the H_2ppz^{2+} ligand (found 37.40, calcd. 37.16%). The exothermic third stage, a loss of $C_6N_2O_7$ of $dipic^{2-}$ residue is observed between 290 and 600 °C with DTG_{max} at 467 and 488 °C (found 35.55, calcd. 35.58%). The final decomposition product was NiO identified by IR spectroscopy (found 10.15%, Calcd 10.28%).

3.4. UV/vis spectrum, magnetic susceptibility and molar conductivity

The electronic absorption spectra of **1**, **2** and **3**, and the free ligand (**4**) were recorded in water and DMSO solutions at a $1 \times 10^{3-}$ M concentration at room temperature. In the UV range, all compounds exhibit strong absorption bands in water solution

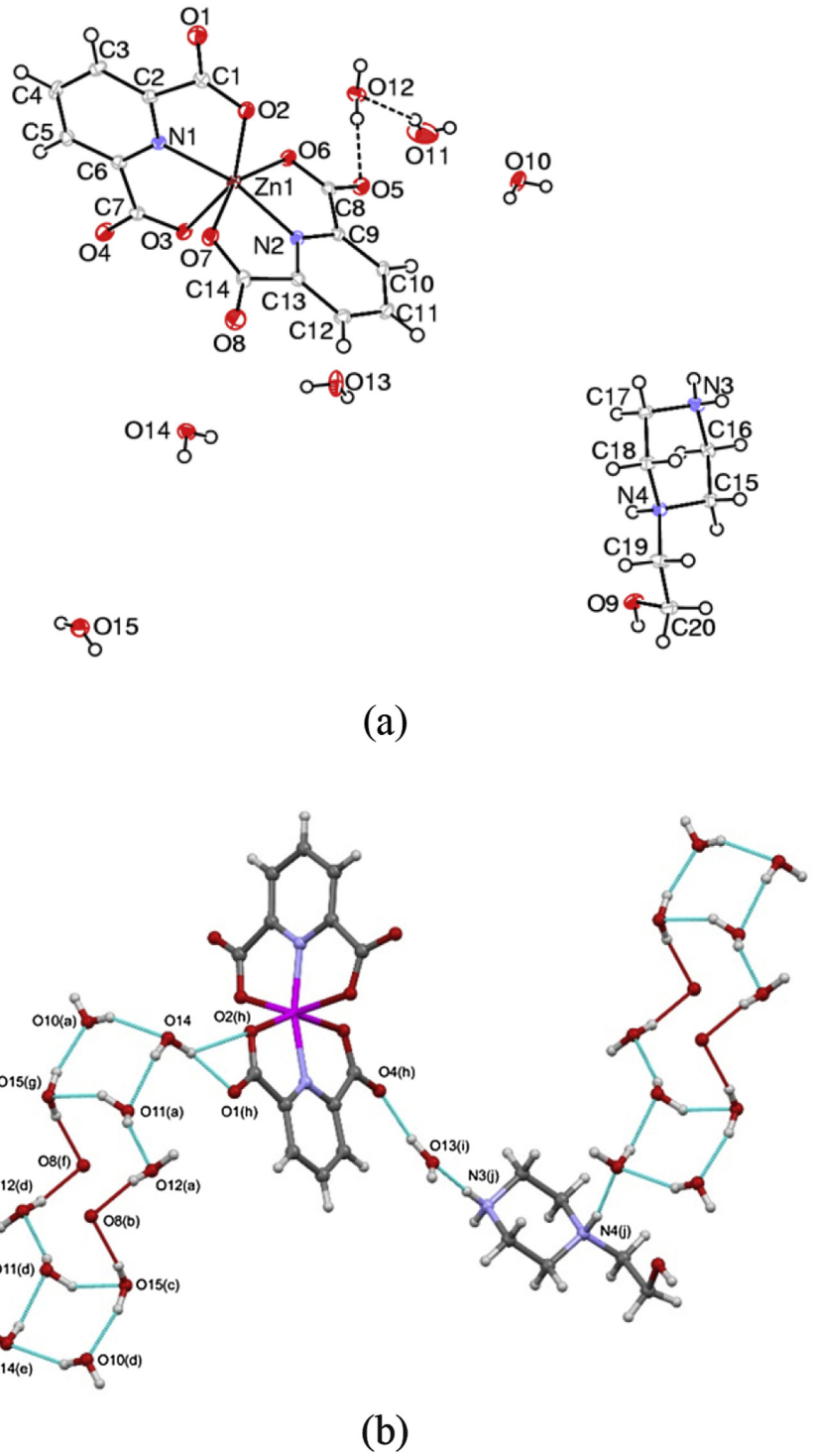

Fig. 3. (a) The molecular structure of compound **3** with the atom-numbering scheme Displacement ellipsoids are drawn at a 50% probability level. The intermolecular O–H···O hydrogen bonds are shown as dashed lines. (b) A view of the dodecanuclear water cluster a: 1 − x,1/2 + y,1/2 − z; b: −1 + x,y,z; c: x,3/2 − y,1/2 + z; d: x,1/2 − y,1/2 + z; e: x − 1,1 − y,1 − z; f: 2 − x,1 − y,1 − z; g: 1 − x,−1/2 + y,1/2 − z; h: 2 − x,1/2 + y,1/2 − z; i: 1 + x,3/2 − y,1/2 + z; j: 1 + x, 1 + y,z.

(280 nm for **1**, 287 nm for **2**, 282 for **3** and 289 and 294 nm for **4**) and in DMSO solution (280 nm for **1**, 287 nm for **2**, 285 nm for **3** and 288 nm for **4**), which can be assigned to intramolecular π–π* transitions. In the visible region, broad absorption bands are observed at 523 and 789 nm in water solution and at 520 and 789 nm in DMSO solution for **1**; these bands are found out for **2** at 874, 892 and 898 nm in water solution and at 798, 818 and 893 nm in DMSO solution which can be assigned to d–d transitions [18]. As expected, d–d transition was not observed for compound **3** due to d^{10} electronic structure of Zn(II) ion (Table S7).

These results are further confirmed by the magnetic susceptibility values. The measured magnetic moment value for **1** is 3.87 B.M., which is consistent with the expected spin-only magnetic moment of d^7 Co(II) system (3.87 B.M.). The magnetic moment of

the Ni(II) compound (**2**) is 2.83 B.M., indicating the presence of two unpaired electrons. This result is in good agreement with a high spin d^8 system in an octahedral environment (2.83 B.M.) [37,38]. As expected, no magnetic moment was observed for the diamagnetic Zn(II) complex in compound **3**.

The conductivity data in DMSO and in water are of 44 and 84.9 Ω^{-1} cm^2 mol^{-1} for **1**, 41 and 64.5 Ω^{-1} cm^2 mol^{-1} for **2**, and 51 and 78.6 Ω^{-1} cm^2 mol^{-1} for **3**, respectively, indicating that the compounds **1**–**3** are ionic [39].

3.5. Biological activity

The compounds **1**–**3** were screened for antibacterial activities along with the free ligands **4**, H_2dipic and ppz (Tables S4 and S5). The minimal inhibition concentration (MIC) and the disc diffusion values of the newly synthesized compounds (**1**–**3**) and free ligands (**4**, H_2dipic and ppz) are shown in Tables S8 and S9, respectively. According to the antimicrobial screening data, while the MIC value of starting compounds (**4** and H_2dipic) exhibited approximately 312.5–625 μg/mL for all studied microorganisms, ppz showed antibacterial activities in the range between 1.562 and 6.250 μL. The newly synthesized compounds **1**–**3** showed a lower antimicrobial effect (4000 μg/mL) for all microorganisms (except *B. subtilis* and clinical *E. Aerogenes* samples with the MIC value more than 4000 μg/mL) than for free ligands (**4** and H_2dipic). According to the specification of the cell wall, the activity of synthesized substances did not change. Therefore, the gram positive or negative bacteria showed similar results. Also, the antimicrobial effectiveness did not differ from clinical isolates (especially clinical isolate *E. coli*, MRSA and their wild-type bacteria). In our previous study, the MIC value of $(H_2ppz)[Cu(dipic)_2]\cdot 6H_2O$ was found to be more than 3000 μg/mL [18].

4. Conclusion

In the present work, three new Co(II) (**1**), Ni(II) (**2**) and Zn(II) (**3**) compounds have been synthesized from the reaction of corresponding metal(II) acetates and proton transfer salt, $(H_2ppz)(Hdipic)_2$, of 2-(piperazin-1-yl)ethanol (ppz) and pyridine-2,6-dicarboxylic acid (H_2dipic). The molecular structure of compounds **1**–**3** consists of one H_2ppz^{2+}cation, one $[M(dipic)_2]^{2-}$ anion and six uncoordinated water molecules. M(II) ions have six coordinated environment comprising two N atoms from two dipic moieties and four O atoms from two carboxylate groups of dipic. Elemental analyses and all measurements show good agreement with the crystal structures. Antimicrobial activities of new compounds $[(H_2ppz)[Co(dipic)_2]\cdot 6H_2O$ (**1**), $[(H_2ppz)[Ni(dipic)_2]\cdot 6H_2O$ (**2**) and $[(H_2ppz)[Zn(dipic)_2]\cdot 6H_2O$ (**3**) against Gram (−) wild type (*E. coli* and *P. aeruginosa*), Gram (+) wild type (*S. aureus, S. epidermidis, B. cereus* and *B. subtilis*) and clinical isolates (*M. morganii, P. vulgaris and E. aeruginosa*) have been studied. MIC values indicate that the synthesized compounds are less effective on bacteria than the related free ligands.

Acknowledgement

This study was supported by a grant (Grant No: 2011-13) received from Dumlupınar University Research Foundation and was carried out at the Department of Chemistry of Dumlupinar University. The authors would like to express their gratitude to the "Medicinal Plants and Medicine Research Center of Anadolu University, Eskişehir" for having received the permission to use the X-ray facility.

Appendix A. Supplementary data

Supplementary data related to this article can be found at http://dx.doi.org/10.1016/j.molstruc.2015.08.015.

References

[1] M.V. Kirillova, M.F.C.G. da Silva, A.M. Kirillov, J.J.R. Fraústo da Silva, A.J.L. Pombeiro, Inorg. Chim. Acta 360 (2006) 506–512.
[2] H.L. Gao, L. Yi, B. Zhao, X.Q. Zhao, P. Cheng, D.Z. Liao, S.P. Yan, Inorg. Chem. 45 (2006) 5980–5988.
[3] L.L. Wen, D.B. Dang, C.Y. Duan, Y.Z. Li, Z.F. Tian, Q.J. Meng, Inorg. Chem. 44 (2005), 7161–7070.
[4] S.K. Ghosh, P.K. Bharadwaj, Inorg. Chem. 44 (2005) 3156–3162.
[5] J.C. MacDonald, T.J.M. Luo, G.T.R. Palmore, Cryst. Growth Des. 4 (2004) 1203–1209.
[6] J.C. MacDonald, P.C. Dorrestein, M.M. Pilley, M.M. Foote, J.L. Lundburg, R.W. Henning, A.J. Schultz, J.L. Manson, J. Am. Chem. Soc. 122 (2000) 11692–11702.
[7] M. Chatterjee, M. Maji, S. Ghosh, T.C.W. Mak, J. Chem. Soc. Dalton Trans. (1998) 3641–3646.
[8] L.C. Nathan, Trends Inorg. Chem. 3 (1993) 415–435.
[9] T.K. Prasad, M.V. Rajasekharan, Cryst. Growth Des. 6 (2006) 488–491.
[10] Y.S. Jiang, G.H. Li, Y. Tian, Z.L. Liao, J.S. Chen, Inorg. Chem. Commun. 9 (2006) 595–598.
[11] S.K. Ghosh, P.K. Bharadwaj, Inorg. Chim. Acta 359 (2006) 1685–1689.
[12] S.K. Ghosh, J. Ribas, P.K. Bharadwaj, Cryst. Growth Des. 5 (2005) 623–629.
[13] S.K. Ghosh, P.K. Bharadwaj, Inorg. Chem. 44 (2005) 5553–5555.
[14] S.K. Ghosh, J. Ribas, P.K. Bharadwaj, Cryst. Eng. Comm. 6 (2004) 250–256.
[15] S.K. Ghosh, P.K. Bharadwaj, Inorg. Chem. 42 (2003) 8250–8254.
[16] M.C. Das, S.B. Maity, P.K. Bharadwaj, Curr. Opin. Solid State Mater. Sci. 13 (2009) 76–90.
[17] B. Zhao, L. Yi, Y. Dai, X.Y. Chen, P. Cheng, D.Z. Liao, S.P. Yan, Z.H. Jiang, Inorg. Chem. 44 (4) (2005) 911–920.
[18] N. Büyükkıdan, C. Yenikaya, H. İlkimen, C. Karahan, C. Darcan, E. Sahin, Russ. J. Coord. Chem. 39 (2013) 96–103.
[19] C. Yenikaya, M. Poyraz, M. Sari, F. Demirci, H. Ilkimen, O. Buyukgungor, Polyhedron 28 (2009) 3526–3532.
[20] A.C. Gonzalez Baro, E.E. Castellano, O.E. Piro, B.S. Parajon Costa, Polyhedron 24 (2005) 49–55.
[21] H. Sakurai, Y. Koyima, Y. Yoshikawa, K. Kawabe, H. Yasui, Coord. Chem. Rev. 226 (2002) 187–198.
[22] O.Z. Yesilel, G. Kastas, C. Darcan, I. Ilker, H. Pasaoglu, O. Buyukgungor, Inorg. Chim. Acta 363 (2010) 1849–1858.
[23] O.Z. Yesilel, A. Mutlu, C. Darcan, O. Buyukgungor, J. Mol. Struct. 964 (2010) 39–46.
[24] E.K. Efthimiadou, A. Karaliota, G. Psomas, Polyhedron 27 (2008) 349–356.
[25] M.M. El-ajaily, F.I. El-moshaty, R.S. El-zweay, A.A. Maihub, Int. J. ChemTech Res. 1 (1) (2009) 80–87.
[26] C. Yenikaya, N. Büyükkıdan, M. Sarı, R. Keşli, H. İlkimen, M. Bülbül, O. Büyükgüngör, J. Coord. Chem. 64 (2011) 3353–3365.
[27] M.A. Neelakantan, S.S. Mariappan, J. Dharmaraja, K. Muthukumaran, Acta Chim. Slov. 57 (1) (2010) 198–205.
[28] S.N. Shukla, P. Gaur, H. Kaur, M. Prasad, R. Mehrotra, R.S. Srıvastava, J. Coord. Chem. 61 (3) (2008) 441–449.
[29] H. İlkimen, C. Yenikaya, M. Sarı, M. Bülbül, E. Tunca, H. Dal, M. ., Baş, J. Inhib. Enzyme Med. Chem. 30 (2) (2015) 195–203.
[30] H. İlkimen, C. Yenikaya, M. Sarı, M. Bülbül, E. Tunca, H. Dal, J. Inhib. Enzyme Med. Chem. 29 (3) (2014) 353–361.
[31] H. İlkimen, C. Yenikaya, M. Sarı, M. Bülbül, E. Tunca, Y. Süzen, Polyhedron 61 (2013) 56–64.
[32] H. İlkimen, C. Yenikaya, M. Sarı, M. Bülbül, M. Aslan, Y. Süzen, J. Inhib. Enzyme Med. Chem. 29 (5) (2014) 695–701.
[33] Bruker SADABS. Madison, Wisconsin, USA: Bruker AXS Inc.; 2005.
[34] G.M. Sheldrick, Acta Cryst. A64 (2008) 112–122.
[35] NCCLS Methods for Dilution Antimicrobial Susceptibility Tests for Bacteria that Grow Aerobically, Approved Standard, Document M7–A7, Wayne (PA, USA): Clinical Laboratory Standards Institute, 2006.
[36] M.C. Das, S.B. Maity, P.K. Bharadwaj, Curr. Opin. Solid State Mater. Sci. 13 (2009) 76–90.
[37] W.J. Geary, Coord. Chem. Rev. 7 (1971) 81–122.
[38] S. Chandra, R. Kumar, Synth. React. Inorg. Met. -Org. Nano-Met. Chem. 35 (2005) 161–170.
[39] P.A. Ajibade, G.A. Kolawole, P. O'Brien, M. Helliwell, J. Raftery, Inorg. Chim. Acta 359 (2006) 3111–3116.